Molecular Assembly of Rubrene on a Metal/Metal Oxide Nanotemplate†

Fabio Cicoira,‡ Jill A. Miwa,‡ Dmitrii F. Perepichka,§ and Federico Rosei*,‡

Centre Énergie Matériaux et Télécommunications, Institut National de la Recherche Scientifique (INRS), Université du Québec, 1650 Boul, Lionel-Boulet, Varennes, QC, CANADA J3X 1S2, and Department of Chemistry, McGill University, 801 Sherbrooke St. West, Montréal, QC, Canada H3A 2K6

Received: July 31, 2007; In Final Form: September 22, 2007

We investigated the adsorption properties and self-assembly of rubrene molecules on the copper oxide nanotemplate formed by high-temperature exposure of Cu(110) to molecular oxygen. Using high-resolution scanning tunneling microscopy under ultrahigh-vacuum conditions, we observed a complex variety of self-assembled motifs, driven by competing effects such as the chemical affinity between the organic molecule and the surface, surface coverage, and spatial confinement of the rubrene molecules within the rows of the template.

Introduction

Nanostructured surfaces have been widely studied during the last decades and are gaining increasing importance in modern science and technology.[1−4] Exciting and promising opportunities rely on the use of nanostructured surfaces as templates for the controlled growth of highly ordered inorganic or organic compounds. Surface nanotemplates are substrates that are artificially or naturally patterned at the nanoscale, where specific functionalities provide surface cues that are able to drive self-assembly.[5] There are several types of surface templates among which the most common are long-range reconstructions,[6−9] step bunching,[10,11] vicinal surfaces,[12] ordered growth from defects,[13,14] inorganic nanomeshes,[15,16] organic porous networks,[17−25] metal−organic coordinated networks,[26,27] and macrocycle monolayers.[28]

A long range reconstruction that results in an interesting one-dimensional nanotemplate is the (2×1) oxygen-induced reconstruction of the Cu(110) surface.[29] The template is formed by exposing the Cu(110) surface to relatively high pressures of oxygen at elevated temperatures under ultrahigh vacuum (UHV) conditions. Early studies on this system revealed that the reaction between chemisorbed oxygen and surface Cu atoms leads to the formation of O−Cu strings running along the [001] direction of the Cu(110) surface. The strings organize in islands separated by two [1$\bar{1}$0] lattice spacings (0.512 nm).[30−32] Under appropriate substrate temperature and oxygen pressure, the islands arrange themselves into stripes running along the [001] direction.[33] The (2×1)O−Cu (oxygen-passivated) stripes are separated by regularly spaced clean copper areas and form a periodic grating. The width of the stripes can be adjusted by varying the oxygen pressure and the substrate temperature during the oxidation process.[8]

The O−Cu nanotemplate can be used to drive highly ordered patterns of organic molecules based on their higher affinity for the clean Cu areas rather than the oxygen passivated stripes. The template represents an ideal tool for studying the self-assembly and the electronic properties of organic molecules because metallic stripes with a width approaching molecular dimensions can be used to explore the effect of spatial confinement on the adsorption geometry and molecular patterning.[7,8,9,34] Moreover, adsorption geometries and self-assembled patterns of organic molecules can be simultaneously studied on two different surfaces, namely the clean and the oxygen-passivated Cu(110).

Rubrene (5,6,11,12-tetraphenyltetracene, $C_{42}H_{28}$) is a model system to study the self-assembly of nonplanar molecules on crystal surfaces. The molecule consists of a tetracene backbone with four phenyl substituents symmetrically attached to the two sides of the backbone (Figure 1a). It is being widely studied for applications in organic electronics, including light-emitting diodes[35−37] and field-effect transistors (FETs).[38−42] The energy level alignment of rubrene thin films on Au(111) has been recently studied and has been shown to depend on film thickness.[43] Single crystals of rubrene exhibit values of the hole field-effect mobility among the highest observed in organic materials ($\sim$15 cm^2/(V s)).[38,39] However, no high mobility FETs could be fabricated from vacuum-deposited or solution-processed thin films. Thin film FETs with mobility of 0.7 cm^2/(V s) were fabricated by melt-processing of an eutectic mixture of rubrene with 5,10-diphenylanthracene.[44] The steric interactions between the phenyl substituents in rubrene result in a significant strain in the molecule which can be released either by twisting the tetracene core (i), as for the gas-phase geometry of rubrene (Figure 1b), or by out-of plane distortion of phenyl substituents (ii), as established by X-ray analysis in rubrene single crystals.[45] The twisting of the tetracene backbone renders the molecule chiral in the gas phase (Figure 1b). The planar conformation provides efficient intermolecular $\pi-\pi$ interactions leading to high mobility whereas the twisted geometry is unfavorable for charge carrier transport. Therefore, understanding the self-assembly of rubrene molecules on various surfaces is of paramount importance to understand the growth of rubrene thin films for organic electronic devices. In situ near edge X-ray absorption fine structure (NEXAFS) studies of rubrene thin films grown on Au(111) and on SiO_2 demonstrated that it retains its twisted geometry in the early stages of growth whereas the planar geometry, characteristic of the crystalline material, is found after deposition of several layers.[46] Scanning tunneling

† Part of the "Giacinto Scoles Festschrift".

* Corresponding author. E-mail: rosei@emt.inrs.ca.
‡ Université du Québec.
§ McGill University.

10.1021/jp076090c CCC: $37.00
Published on Web 11/06/2007

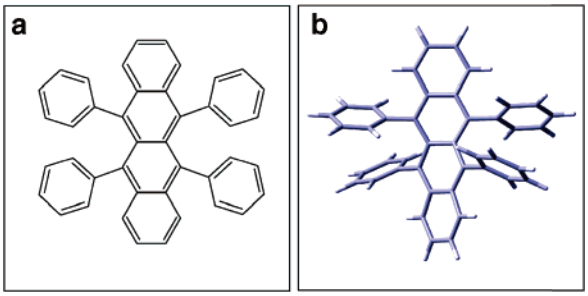

Figure 1. (a) Molecular structure of rubrene and (b) 3-dimensional rendering of rubrene in the gas phase as calculated with density functional theory (B3LYP/6-31G(d)).

microscopy (STM) studies of rubrene on Au(111) carried out at 5 K demonstrated that the twisted conformation of the molecule and its chirality are retained upon physisorption and can be exploited to drive the assembly of exotic chiral hierarchical supramolecular structures.[47] STM investigations were carried out also on single-crystal surfaces in ambient air and revealed a herringbone-like motif similar to that found in the bulk.[48]

In this paper, we investigate the adsorption and self-assembly properties of rubrene molecules on the O−Cu nanotemplate by *in situ* high-resolution STM in UHV. We show that rubrene adsorbs preferentially on the clean Cu(110) stripes. Coverage of the stripes proceeds after their saturation with the formation of multilayers. Due to the spatial confinement on the nanometric Cu(110) stripes of the template, rubrene molecules are found to form a different arrangement than that formed on pristine Cu(110).

Experimental Section

STM observations were carried out in situ with an Omicron variable temperature (VT) UHV−STM with a base pressure $<5 \times 10^{-11}$ mbar. The Cu(110) single crystals (Matek GmbH) were cleaned by repeated 600 eV Ar^+ sputtering and annealing (∼825 K) cycles. The O−Cu nanotemplate was prepared by dosing 0.5−1.0 langmuir, where 1 langmuir $= 10^{-6}$ Torr s^{-1}, of oxygen via a precision leak valve onto the Cu(110) surface held at 623 K. Higher doses (∼5 langmuirs) at the same temperature resulted in an almost completely (2×1) oxygen reconstructed surface. Rubrene (Aldrich, purity 99%) was evaporated from a well degassed Knudsen cell at temperatures ranging from 430 to 450 K on surfaces held at room temperature at a pressure ranging between 5×10^{-10} and 2×10^{-9} mbar. The STM measurements were performed at room temperature (RT) with a chemically etched W tip. In general, imaging of adsorbed rubrene molecules was carried out at ∼−2 V and ∼0.3 nA. A negative polarity indicates that the sample is biased negatively with respect to the tip. All images were acquired on the topographic channel and later processed using WSxM software.[49] Packing densities for the self-assembled patterns were estimated from several STM images.

Results and Discussion

Self-Assembly of Rubrene on Pristine Cu(110). To understand the effects of the O−Cu nanotemplate on rubrene adsorption and self-assembly, we first briefly present data relative to its adsorption on the pristine Cu(110) surface. The self-assembly of rubrene on Cu(110) leads to the two structures (A and B) shown in Figure 2a,b. Rubrene molecules within the self-assembled motifs are imaged as four bright lobes, corresponding to the four phenyl substituents, which surround a

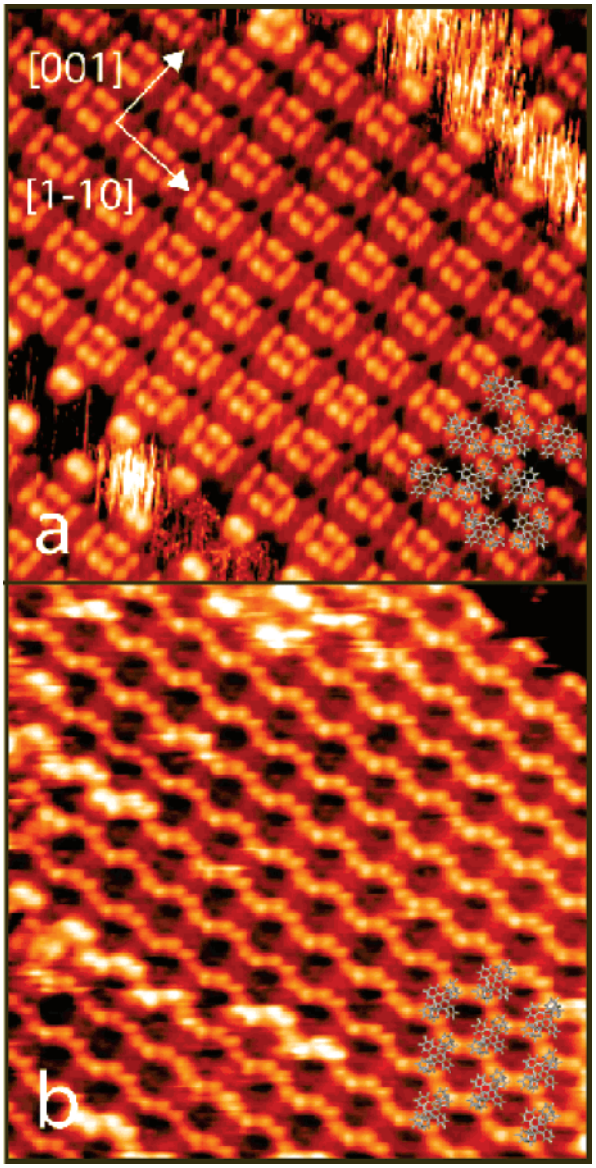

Figure 2. Rubrene adsorption on Cu(110). 15×15 nm^2 STM images of (a) structure A and (b) structure B. Tunneling parameters: $I_t = 0.3$ nA, $V_t = -1.9$ V (a); $I_t = 0.34$ nA, $V_t = -0.53$ V (b).

dimmer region, corresponding to the tetracene backbone.[50] The two structures are characterized by a different orientation of the molecules with respect to the underlying surface, as highlighted by the superimposed molecular models. Structure A can be represented as a sequence of rows running along the [001] direction, where all the molecules are oriented with the tetracene backbone lying alternatively along the [001] or [1$\bar{1}$0] direction. In structure B, all the molecules are oriented with their tetracene backbone parallel to the [1$\bar{1}$0] direction. Adjacent molecules in the [001] direction are shifted with respect to each other by approximately one molecular unit (∼1 nm). The packing density is about 0.60 molecules nm^{-2} for structure A and about 0.45 molecules nm^{-2} for structure B. At equilibrium, the two structures are equally distributed across the surface. The self-assembly of rubrene on pristine low index copper surfaces ((110) and (001)) will be discussed in more detail in a forthcoming paper.[51]

Self-Assembly of Rubrene on the O−Cu Template. An STM image of the O−Cu nanotemplate used for this study is shown in Figure 3a. It consists of a nanograting in which the stripes of copper and (2×1)O−Cu have a width ranging between

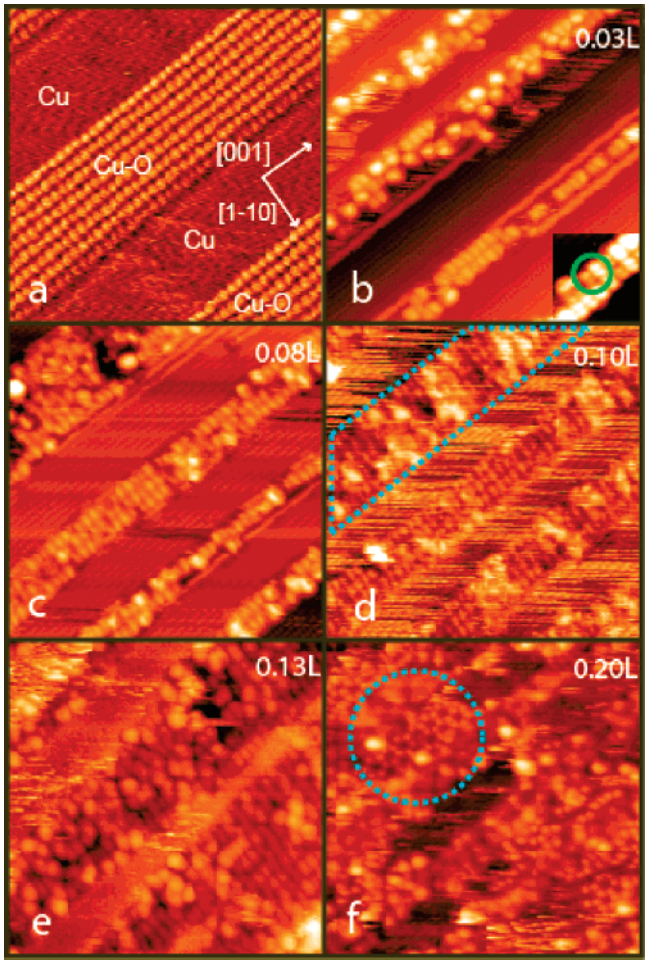

Figure 3. Self-assembly of rubrene on the O−Cu nanotemplate: 12.6 × 12.6 nm^2 STM images of the O−Cu nanotemplate (a); 26 × 26 nm^2 STM images (b)−(f) of the O−Cu nanotemplate exposed to increasing rubrene doses [0.03 langmuir (b), 0.08 langmuir (c), 0.10 langmuir (d), 0.13 langmuir (e), 0.20 langmuir (f)]. Tunneling parameters: $V_t = 1.05$ V, $I_t = 1.03$ nA (a); 2.09 V, 0.31 nA (b); 2.09 V, 0.38 nA (c); $V_t = 2.0$ V, $I_t = 0.32$ nA (d); $V_t = -2.22$ V, $I_t = 0.36$ nA (e); $V_t = 2.62$ V, $I_t = 0.28$ nA (f). Inset of Figure 3b: 5 × 5 nm, $V_t = -2.27$ V, $I_t = 0.25$ nA.

5 and 10 nm. The O−Cu stripes, which develop along the [001] direction and form a (2×1) structure, are imaged with atomic resolution.[52] The coexistence of hydrophilic (O−Cu) and lipophilic (Cu) surfaces in the nanotemplate represents a good model for FET devices, where the dissimilar adsorption properties of the organic semiconductor on metal electrodes and gate dielectric, and at the interface between them, is a key issue for device performance.

STM images of rubrene adsorbed on the nanotemplate were obtained for increasing rubrene coverages (Figure 3b−f). For an initial dose of 0.03 langmuir (Figure 3b), rubrene adsorbs exclusively on the bare copper stripes and decorates the Cu step edges (as seen in the center of Figure 3b). This result is in agreement with previous observations on other π-conjugated organic molecules on the same surface. This is explained by the higher affinity of the π-conjugated core of the molecules for the metallic copper regions, compared to the O−Cu ones.[7−9] The highly polarizable metal surface provides for stronger van der Waals interactions than the highly polar, and thus weakly polarizable, O−Cu surface. A rubrene molecule adsorbed on a copper stripe of the template is highlighted in the inset of Figure 3b. As on pristine Cu(110) (refer to Figure 2), each rubrene molecule appears as four lobes surrounding a dimmer region. The molecules are adsorbed with the backbone oriented along the [1$\bar{1}$0] direction and self-assemble into a closed packed structure. Depending on the width of the Cu stripes, rubrene islands can be as narrow as one or two molecular units (Figure 3b). Increasing the coverage to 0.08 langmuir leads to saturation of the copper stripes (Figure 3c). A comparison between Figure 2 and Figure 3 (panels b and c) reveals that the self-assembled motif formed by rubrene on the copper stripes of the nanotemplate is different than those formed on the pristine Cu(110) surface. Structure A does not form because the great majority (more than 90%) of the molecules are aligned with the long axis of the tetracene backbone along the [1$\bar{1}$0] direction. The structure formed on the template also differs from structure B, although the molecules are aligned along the [1$\bar{1}$0] direction of Cu(110). A close inspection of Figures 2b and 3b reveals that the main difference between the two structures is the molecular packing. On clean Cu(110) the molecules packed along the [1$\bar{1}$0] direction are spaced by approximately one molecular unit, which results in the open structure shown in Figure 2b. On the nanotemplate, the molecules are packed side-by-side forming a more compact structure. The evaluation of the packing density of rubrene on the copper stripes of the template is not very accurate, because the values could only be averaged over small areas. However we estimate a packing density of ∼0.55 molecules nm^{-2}, as compared to ∼0.45 molecules nm^{-2} of structure B. These results demonstrate that confining the adsorption into a region a few nanometers wide, i.e., close to the molecular dimensions, can significantly modify the self-assembly properties of organic molecules. The spatial confinement effect is possibly also due to the presence of lateral substituents with the consequent nonplanarity of rubrene. In agreement with this hypothesis, the spatial confinement effect was not observed for the linear and planar molecule α-quinquethiophene deposited on the same template.[9] Upon further increase of coverage to 0.10 and 0.13 langmuir (Figure 3d,e), the Cu stripes are progressively covered by several rubrene layers, as highlighted by the blue dashed lines in Figure 3d. Raster noise (visible in Figure 3d,e) appears on the O−Cu regions, indicating the presence of rubrene molecules diffusing on the surface. Exposure to a significantly higher dose of rubrene (0.20 langmuir) resulted in the adsorption on the O−Cu regions of the nanotemplate. As highlighted by the circle in Figure 3f, in this latter case we observe a new, flower-like pattern, different from those observed both on pristine Cu(110) and on the copper stripes of the template. The main difference between this structure and those found on Cu(110) is that the backbones of the molecules are not oriented along the high-symmetry surface directions.

Self-Assembly of Rubrene on the (2×1)O−Cu Surface. To gain insight into the flower-like structure observed on the O−Cu regions of the nanotemplate, we studied rubrene adsorption on an almost completely (2×1) reconstructed O−Cu surface (where the width of O−Cu stripes exceeded 100 nm). As shown in Figure 4b,c, we found two different coexisting structures, equally distributed on the surface: a new row-like structure (Figure 4b) and the flower-like structure previously observed on the nanotemplate (Figure 4c).

The row-like structure is similar to that observed on the bare copper stripes of the template. The molecules appear as two lobes and have their backbones oriented perpendicularly to the [001] direction of the Cu(110) surface (see superimposed molecular models). On the oxygenated surface the phenyl substituents could not be individually resolved, despite numerous attempts. Possible explanations could be (i) lower contrast (and

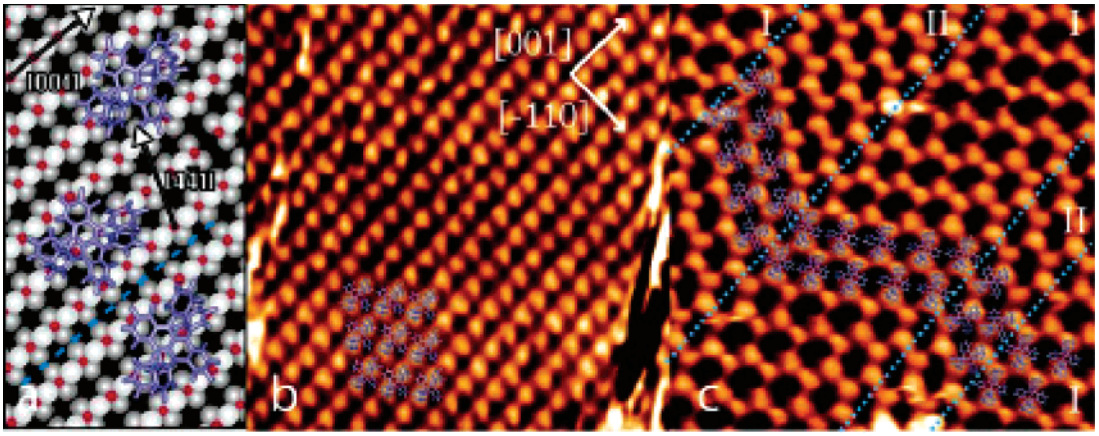

Figure 4. Rubrene self-assembly on a O−Cu surface. (a) Molecular model for the adsorption geometry of individual molecules for the row-like (upper portion) and the flower-like (lower portion) structure. The white circles represent Cu atoms and the red circles O atoms. (b) Row-like structure. 13.4 × 13.4 nm^2, $V_t = 3.14$ V, $I_t = 0.19$ nA. The vectors indicate Miller indices for the underlying Cu lattice. (c) Flower-like structure. 13.4 × 13.4 nm^2, $V_t = -1.9$ V, $I_t = 0.3$ nA.

therefore poorer resolution) resulting from an adsorption state on a slightly more complex surface, or (ii) lower resolution due to a convolution effect from rapid switching between equivalent twisted geometries. Investigations on other Cu surfaces as well as density functional calculations are in progress to clarify this issue.[51] A tentative model for the adsorption geometry is illustrated in the upper portion of Figure 4a. The molecules assemble side by side into a tightly packed structure forming rows running in the same direction as the O−Cu stripes (i.e., the [001] direction of the pristine Cu surface). This structure has a packing density of ∼0.75 molecules nm^{-2}. The intra-row and the inter-row periodicities are ∼1 nm, and adjacent rows are shifted by ∼0.65 nm with respect to one another, thereby increasing the packing efficiency of this structure. The unit cell for this molecular arrangement, with vectors $\mathbf{a}_1$ and $\mathbf{b}_1$, is described in real space matrix notation as

$$\begin{pmatrix} \vec{a}_1 \\ \vec{b}_1 \end{pmatrix} = \begin{pmatrix} 4 & 2 \\ 0 & 4 \end{pmatrix} \begin{pmatrix} \vec{a}_s \\ \vec{b}_s \end{pmatrix}$$

where $|\vec{a}_s| = 0.256$ nm and $|\vec{b}_s| = 0.361$ nm and correspond to the underlying lattice vectors of the Cu(110) surface. The orientation of rubrene molecules along the $[1\bar{1}0]$ direction on the O−Cu surface reveals that, despite the weak molecule/substrate interactions, the substrate symmetry still plays a role in the formation of the self-assembled pattern. Such a molecular orientation was not unexpected as the lattice spacing along the direction of the O−Cu stripes is twice the $[1\bar{1}0]$ lattice spacing of Cu(110). This suggests a similar commensurability of rubrene with the two different surfaces. In the flower-like structure, rubrene molecules exhibit an unusual arrangement (Figure 4c). The molecules are not oriented along the high-symmetry directions of the surface. The individual molecules adsorb in a "tilted" geometry. The tilting here is intended as an in-plane rotation with respect to the [001] direction of the surface. The imaged phenyl substituents are aligned along a line that forms an angle of ∼53° with respect to the [001] direction of the underlying copper lattice. If we assume that the molecule is not completely distorted upon adsorption and the phenyl substituents are positioned roughly as shown in Figure 1b, the tetracene backbone will be aligned along the $[4\bar{4}1]$ direction of the surface. Due to the symmetry of the O−Cu surface, rubrene molecules should also adsorb with their backbone aligned along the equivalent $[\bar{4}41]$ direction. These two orientations are illustrated in the lower portion of the tentative model reported in Figure 4a, where the dashed blue line represents a mirror plane. Figure 4c shows a region of the O−Cu surface covered by the characteristic flower-like structure where the equivalent rubrene adsorption orientations phase-separate into reflection twin domains, labeled I and II. The dashed blue lines mark the domain boundaries. Molecular models are superimposed on the image to clarify the two equivalent adsorption geometries. Rows of rubrene run along the [001] direction of the surface giving a unit cell:

$$\begin{pmatrix} \vec{a}_1 \\ \vec{b}_1 \end{pmatrix} = \begin{pmatrix} 4 & 2 \\ 0 & 4 \end{pmatrix} \begin{pmatrix} \vec{a}_s \\ \vec{b}_s \end{pmatrix}$$

Domain II is the same as domain I but reflected through the (001) axis, so its matrix is

$$\begin{pmatrix} \vec{a}_1 \\ \vec{b}_1 \end{pmatrix} = \begin{pmatrix} -4 & 2 \\ 0 & 4 \end{pmatrix} \begin{pmatrix} \vec{a}_s \\ \vec{b}_s \end{pmatrix}$$

Ultimately, the overall adlayer structure is quite similar to a skewed version of structure B on the pristine Cu(110) surface (see Figure 2b). The flower-like structure is also similar to the row-like structure observed on the same surface with increased inter- and intra-row spacings. The packing density for this structure was determined to be about 0.63 molecules nm^{-2}.

Our results show that upon adsorption on a template, self-assembly is governed by a competition between intermolecular interactions, close packing requirements and the available binding sites on the surface. Therefore upon adsorption on a nanopatterned surface even a fairly simple molecule can give a complex variety of self-assembled motifs, with strong implications on the growth of organic thin films. Indeed, the crystal structure of an organic single crystal or thin film on a smooth SiO_2 surface (which is often used as a model system in studying the properties of the active layer of hybrid/inorganic devices) may not give a complete picture of molecular packing in the real device. We have shown that a fairly realistic picture is provided by adsorption on the nanotemplate, where electrode-like (Cu) and dielectric like (O−Cu) surfaces coexist.

Conclusions

We have shown that an O−Cu nanotemplate on the Cu(110) surface can be used to drive the self-assembly of rubrene into a variety of highly ordered patterns. At low coverage, due to the high affinity of the π-electron rich molecular backbone for

the metallic surface, rubrene molecules adsorb preferentially on the bare copper stripes of the nanotemplate. Here we observe a self-assembled structure different from those observed on the pristine Cu(110) surface: the molecules are disposed side by side possibly as a consequence of the spatial confinement into the nanometric stripes of the template. At higher degrees of coverage, after the formation of molecular multilayers on the metallic stripes, rubrene adsorbs on the O−Cu regions, forming a flower-like pattern. Subsequent observations of rubrene self-assembly on an almost completely O−(2×1) reconstructed Cu-(110) surface reveal the coexistence of two self-assembled patterns, characterized by a different alignment of the molecular backbone with respect to the substrate surface and a different packing density.

The O−Cu nanotemplate allows for simultaneous investigations of the adsorption geometries on two different surfaces at the nanoscale. These results contribute to the understanding of the adsorption properties of rubrene on templated surfaces and pave the way for the use of the O−Cu template to study the adsorption and self-assembly of more complex nonplanar molecules such as biomolecules, metallo-organic complexes and nonplanar metalloporphyrins.

Acknowledgment. F.C. and J.A.M. contributed equally to this work. F.R. acknowledges startup funds from INRS. F.C. acknowledges CBIE for partial financial support. We thank Clara Santato for a critical reading of the manuscript and Josh Lipton-Duffin for helpful discussions. F.R. and D.F.P. are funded by NSERC of Canada. F.R. is grateful to FQRNT and the Canada Research Chairs program for partial salary support.

References and Notes

(1) Barth, J. V. *Annu. Rev. Phys. Chem.* **2007**, *58*, 375.
(2) Barth, J. V.; Costantini, G.; Kern, K. *Nature* **2005**, *437*, 29.
(3) Rosei, F. *J. Phys.: Condens. Matter* **2004**, *16*, S1373.
(4) Rosei, F.; Schunack, M.; Naitoh, Y.; Jiang, P.; Gourdon, A.; Laegsgaard, E.; Stensgaard, I.; Joachim, C.; Besenbacher, F. *Prog. Surf. Sci.* **2003**, *71*, 95.
(5) Cicoira, F.; Rosei, F. *Surf. Sci.* **2006**, *600*, 1.
(6) Yokoyama, T; Yokoyama, S.; Kamikado, T.; Okuno, Y.; Mashiko, S.; *Nature* **2001**, *413*, 619.
(7) Pedersen, M. Ø.; Murray, P. W. H.; Lægsgaard, E.; Stensgaard, I.; Besenbacher, F. *Surf. Sci.* **1997**, *389*, 300.
(8) Otero, R.; Naitoh, Y.; Rosei, F.; Jiang, P.; Thostrup, P.; Gourdon, A.; Laegsgaard, E.; Stensgaard, I.; Joachim, C.; Besenbacher, F. *Angew. Chem. Int. Ed.* **2004**, *43*, 2092.
(9) Cicoira, F.; Miwa, J. A.; Melucci, M.; Barbarella, G.; Rosei, F. *Small* **2006**, *2*, 1366.
(10) Sgarlata, A.; Szkutnik, P. D.; Balzarotti, A.; Motta, N.; Rosei, F. *Appl. Phys. Lett.* **2003**, *83*, 4002.
(11) Men, F. K.; Liu, F.; Wang, P. J.; Chen, C. H.; Cheng, D. L.; Lin, J. L.; Himpsel, F. J. *Phys. Rev. Lett.* **2002**, *88*, 096105.
(12) Néel, N.; Kröger. J.; Berndt, R. *Adv. Mater.* **2006**, *18*, 174.
(13) Miwa, J. A.; Eves, B. J.; Rosei, F.; Lopinski, G. P. *J. Phys. Chem. B* **2005**, *109*, 20055.
(14) Lopinski, G. P.; Wayner, D. D. M.; Wolkow, R. A. *Nature* **2000**, *406*, 48.
(15) Chen, W.; Zhang, H. L.; Xu, H.; Tok, E. S.; Loh, K. P.; Wee, A. T. S. *J. Phys. Chem. B* **2006**, *110*, 21873.
(16) Corso, M.; Auwärter, W.; Muntwiler, M.; Tamai, A.; Greber, T.; Osterwalder, J. *Science* **2004**, *303*, 217.
(17) Griessl, S. J. H.; Lackinger, M.; Edelwirth, M.; Hietschold, M.; Heckl, W. M. *Single Mol.* **2002**, *3*, 25.
(18) Dmitriev, A.; Lin, N.; Weckesser, J.; Barth, J. V.; Kern, K. *J. Phys. Chem. B* **2002**, *106*, 6907.
(19) Griessl, S. J. H.; Lackinger, M.; Jamitzki, F.; Markert, T.; Hietschold, M.; Heckl, W. M. *Langmuir* **2004**, *20*, 9403.
(20) Nath, K. G.; Ivasenko, A.; Miwa, J. A.; Dang, H.; Wuest, J. D.; Nanci, A.; Perepichka, D. F.; Rosei, F. *J. Am. Chem. Soc.* **2006**, *128*, 4212.
(21) Theobald, J. A.; Oxtoby, N. S.; Phillips, M. A.; Champness, N. R.; Beton, P. H. *Nature* **2003**, *424*, 1029.
(22) Staniec, P. A.; Perdigao, L. M. A.; Rogers, B. L.; Champness, N. R.; Beton, P. H. *J. Phys. Chem. C* **2007**, *111*, 886.
(23) Perdigão, L. M. A.; Champness N. R.; Beton P. H. *Chem. Commun.* **2006**, 538.
(24) Ruben, M.; Payer, D.; Landa, A.; Comisso, A.; Gattinoni, C.; Lin, N.; Collin. J. P.; Sauvage, J. P.; De Vita, A.; Kern, K. *J. Am. Chem. Soc.* **2006**, *128*, 15644.
(25) Pawin, G.; Wong, K. L.; Kwon, K. Y.; Bartels, L. *Science* **2006**, *313*, 961.
(26) Clair, S.; Pons, S.; Brune, H.; Kern, K.; Barth, J. V. *Angew. Chem., Int. Ed.* **2005**, *44*, 7294.
(27) Stepanow, S.; Lin, N.; Barth, J. V.; Kern, K. *Chem. Commun*. **2006**, 2153.
(28) Mena-Osteritz, E.; Bäuerle, P. *Adv. Mater*. **2006**, *18*, 447.
(29) Ertl, G. *Surf. Sci.* **1967**, *6*, 208.
(30) Jensen, F.; Besenbacher, F.; Laesgaard, E.; Stensgaard, I. *Phys. Rev. B* **1990**, *41*, 10233.
(31) Coulman, D. J.; Wintterlin, J.; Behm, R. J.; Ertl, G. *Phys. Rev. Lett.* **1990**, *64*, 1761.
(32) Besenbacher, F.; Jensen, F.; Lægsgaard, E.; Mortensen, K.; Stensgaard, I. *J. Vac. Sci. Technol. B* **1991**, *9*, 874.
(33) Kern, K.; Niheus, H.; Schatz, A.; Zeppenfeld, P.; Goerge, J.; Comsa, G. *Phys. Rev. Lett*. **1991**, *67*, 855.
(34) Koller, G.; Winter, B.; Oehzelt, M.; Ivanco, J.; Netzer, F. P.; Ramsey, M. G. *Org. Eectron.* **2007**, *8*, 63.
(35) Sakamoto, G.; Adachi, C.; Koyama, T.; Taniguchi, Y.; Merritt, C. D.; Murata, H.; Kafafi, Z. H. *Appl. Phys. Lett.* **1999**, *75*, 766.
(36) Aziz, H.; Popovic, Z. D. *Appl. Phys. Lett.* **2002**, *80*, 2180.
(37) Li, G.; Shinar, J. *Appl. Phys. Lett.* **2003**, *83*, 5360.
(38) Sundar, V. C.; Zaumseil, J.; Podzorov, V.; Menard, E.; Willett, R. L.; Someya, T.; Gershenson, M. E.; Rogers, J. A. *Science* **2004**, *303*, 1644.
(39) Podzorov, V.; Menard, E.; Borissov, A.; Kiryukhin, V.; Rogers, J. A.; Gershenson, M. E. *Phys. Rev. Lett.* **2004**, *93*, 086602.
(40) Takeya, J.; Yamagishi, M.; Tominari, J.; Hirahara, R.; Nakazawa, Y.; Nishikawa, T.; Kawase, T.; Shimoda, T.; Ogawa, S. *Appl. Phys. Lett.* **2007**, *90*, 102120.
(41) Briseno, A.; Mannsfeld, S. C. B.; Ling, M. M.; Liu, S.; Tseng, R. J.; Reese, C.; Roberts, M. E.; Yang, Y.; Wudl, F.; Bao, Z. *Nature* **2006**, *444*, 913.
(42) Takahashi, T.; Takenobu, T.; Takeya, J.; Iwasa, Y. *Appl. Phys. Lett.* **2006**, *88*, 033505.
(43) Wang, L.; Chen. S.; Liu, L.; Qi, D.; Gao, X.; Wee, A. T. S. *Appl. Phys. Lett.* **2007**, *90*, 132121.
(44) Stingelin-Stutzmann, N.; Smits, E.; Wondergen, H.; Tanase, C.; Blom, P.; Smith, P.; De Leeuw, D. *Nature Mater.* **2005**, *4*, 601.
(45) Jurchescu, O. D.; Meetsma, A.; Palstra, T. T. M. *Acta Crystallogr.* **2006**, *B62*, 330.
(46) Käfer, D.; Witte, G. *Phys. Chem. Chem. Phys.* **2005**, *7*, 2850.
(47) Blüm, M. C.; Ćavar, E.; Pivetta, M.; Patthey. F.; Schneider, W. D. *Angew. Chem., Int. Ed.* **2005**, *44*, 5334.
(48) Menard, E.; Marchenko, A.; Podzorov, V.; Gershenson, M. E.; Fichou, D.; Rogers, J. A. *Adv. Mater.* **2006**, *18*, 1552.
(49) Horcas, I.; Fernandez, R.; Gomez-Rodriguez, J. M.; Colchero, J.; Gomez-Herrero, J.; Baro, A. M. *Rev. Sci. Instrum.* **2007**, *78*, 013705.
(50) In light of an expected twisted adsorption geometry, the most interesting aspect is the uniformity or lack of contrast within single rubrene molecules. It is possible that the molecule−surface interaction is substantially weak to allow for a switching of the molecule between energetically equivalent twisted geometries. The switching may occur at a rate faster than the STM image acquisition time, resulting in an averaging out, and thus uniform, appearance of the features. A similar phenomenon has been observed for silicon dimers of the Si(100) surface as reported by: Hata, K.; Sainoo, Y.; Shigekawa, H. *Phys. Rev. Lett.* **2001**, *86*, 3084. Pennac, Y.; Horn von Hoegen, M.; Zhu, X.; Fortin, D. C.; Freeman M. R. *Phys. Rev. Lett.* **2006**, *96*, 026102.
(51) Miwa, J. A.; Cicoira, F.; Bedwani, S.; Lipton-Duffin, J.; Perepichka D. F.; Rochefort A.; Rosei, F. Manuscript in preparation.
(52) The lattice directions refer to the pristine Cu(110) surface.